Supplementary Information

Outstanding capacity assimilated from LMNO flexible cathode materials deposited on the CNT wrapped carbon fibers for flexible lithium ion batteries

Abhilash Karuthedath Parameswaran[a,*], Lukáš Děkanovský [a], Vlastimil Mazánek[a], Sivaraj Pazhaniswamy[b], Zdenek Sofer[a,*]

[a] Department of Inorganic Chemistry, University of Chemistry and Technology Prague, Technická 5, 166 28 Prague 6, Czech Republic

[b] Bavarian Center for Battery Technology, Macromolecular Chemistry II, University of Bayreuth, Universitätsstrasse 30, 95440, Bayreuth, Germany

*Corresponding authors: karuthea@vscht.cz (K.P.A) & Zdenek.Sofer@vscht.cz (Z.S)

S1. Experimental section

S.1.1. Preparation of $Li_2(Mn_x,Ni_{(1-x)})O_3$ (LRMNO) nanoparticles

The LRMNO nanoparticles were prepared by a solution mixing of lithium carbonate (Li_2CO_3, Sigma Aldrich, 99%), manganese dioxide (MnO_2, Sigma Aldrich, 99%), nickel nitrate hexahydrate ($Ni(NO_3)_2.6H_2O$, Sigma Aldrich, 99%). The stoichiometric ($Li_2(Mn_{0.75}Ni_{0.25})O_3$, $Li_2(Mn_{0.66}Ni_{0.33})O_3$, $Li_2(Mn_{0.50}Ni_{0.50})O_3$: other alternate compositions results in poor electrochemical performances) amounts of Li_2CO_3, MnO_2 and $Ni(NO_3)_2.6H_2O$ were thoroughly mixed in a beaker containing 100 mL of de-ionized water using a magnetic stirrer. The resultant mixture was heated in a furnace at 120 °C for two hours. The resultant mixture was ground in a mortar and heated at 750 °C for 22 h for an ideal composition. Here, it should be noted that a variety of the Li-rich manganese nickel oxide compositions could be formed. The present study attempted to prepare such compositions, which properly maintain the structure of Li_2MnO_3 – a monoclinic-layered pattern with the space group C2/m (PDF#: 01-0841634). To achieve this, the Ni to Mn ratio and the calcination temperature (700 to 900 °C)

have been varied in regular manner to get the optimum composition. The composition with stoichiometry $Li_2(Mn_{0.5}Ni_{0.5})O_3$ prepared at 750 °C retains the desired composition of LRMNO nanoparticles with exceptional electrochemical properties.

S.1.2. The CVD growth of 3D-CNT wrapped carbon fibers

The flexible carbon fibers (Kynar carbon fabrics Europa GmbH ACC-5052 (15)) have been well cleaned in strong acidic medium with a heating at 60 °C for 2 hrs. The fabrics has been dried and plasma treated for 10 min. The CNT growth on carbon fabrics was carried out by a controlled Chemical Vapour Deposition (CVD) technique. The carbon fabrics cut into 3×3 cm^2 area pieces have been well sprinkled with the dispersed solution of Pd nanoparticles (catalysts) with 5 nm size and dried at room temperature for 10 minutes. The carbon fabrics were placed at the middle position of the furnace on a quartz boat to maintain uniform heating. Keeping the CVD furnace pressure at low pressure (10 kPa), the reactor was heated to 450 °C in Ar atmosphere, then replaced Ar with H_2 at a flow of 100 mL/min and kept at 450 °C for 30 min to activate the catalyst. The temperature inside the reactor was subsequently raised to 750 °C in Ar atmosphere and the CNTs were formed directly on the surface of the carbon fabrics by introduction of a mixture gas consisting of CH_4, H_2, and Ar for two hours. The feeding rates of these gases were set to 6, 6, and 12 mL/min, respectively. At the end of the feeding period, the gas was replaced by Ar until the reactor was cooled to ambient temperature. After cooling, the uniformly CNT wrapped carbon fabrics can be taken out and used for the deposition of nano-LRMNO.

S.1.3. Spray coating of LRMNO nanoparticles on CNT wrapped carbon fabrics

The spray coating has been identified as a viable technique which is highly suitable for a scale up at the industrial level. The uniform slurry has been prepared using the LRMNO

nanoparticles (active material 85%), PVdF (binder 10%) and carbon black (additive 5%) in N-methylpyrrolidone (NMP) solvent. The mixture has been stirred well overnight using a magnetic stirrer and subsequently loaded into the airbrush spray coater. The mixture can be uniformly sprayed onto the surface of the CVD grown CNT-wrapped carbon fabrics placed on a sheet of paper. In order to reduce the surface energy of the 3D CVD-grown CNT fabrics surface, the fabrics were treated by oxygen plasma for 5 min to improve the wettability of its surface before the spray-coating. The oxygen plasma was produced using a RF generator, operating at 300 W. In order to avoid the particle agglomeration on the surfaces, the slurry has been filtered using a vacuum filtration. The flow rate and the nozzle width can be properly adjusted for a uniform coating without any non-uniform agglomerations over the surface. For this, before attempting on the 3D surface, the film uniformity has been investigated on a planar surface. The LRMNO spray-coated CNT carbon fabrics can be used as an electrode for the battery assembly after drying in an oven at 60 °C. In order to compare the effect of 3D CNT on the surface of carbon fabrics, the LRMNO nanoparticles have also been sprayed onto carbon fabrics without a CVD-CNT coating.

S.1.4. Material characterization

The prepared LRMNO nanoparticles and LRMNO nanoparticles spray-coated onto a CVD grown CNT-wrapped carbon fabrics (termed as: LRMNO@CNT-CC) and LRMNO nanoparticles spray-coated onto carbon fabrics (without CVD-grown CNT) (termed as: LRMNO@CC) have been subjected to structural, morphological and electrochemical characterizations to verify their cathode and fuel cell performances. The samples were analysed using X-ray powder diffraction (XRD, Bruker-AXS D8 Discoverer), by Scanning Electron Microscopy (Tescan Lyra-3). The elemental analysis along with the surface mapping have been determined using Energy dispersive X-ray analysis technique associated with the SEM microscope. The high-resolution transmission electron microscopy (FETEM, JEOL 220 FS)

has been utilized to analyse the explicit morphological features and the microstructure of the LRMNO nanoparticles prepared by the solution route. A single string of carbon fabrics has been taken from the LRMNO@CC and LRMNO@CNT-CC samples to verify the morphological features using the Scanning Transmission Electron Microscopy (STEM-attached to the SEM Tescan Lyra-3). Raman spectra have been recorded using the Renishaw inVia confocal micro-Raman Spectroscope in backscattering geometry with a CCD detector, 532nm DPSS laser and 20x lens. The X-ray photoelectron spectroscopy (XPS) analysis of the LRMNO nanopowder has been carried out by SPEC spectrometer using the XR 50 MF monochromatic X-ray radiation source (1486.7 eV) and the Phoibos 150 2D CCD hemispherical analyser. The pressure inside the chamber was set up lower than 5×10^{-10} mbar during the measurements. Wide scan surveys were obtained at Ep = 80 eV, with subsequent high-resolution scans of the desired core lines were carried out at Ep = 50 eV with a step acquisition of 0.1eV. The binding energy values were corrected to the energy of the carbon C1s peak at 285 eV. The electrochemical characterization of the samples has been carried by fabricating the coin cell (CR-2025) using the LRMNO@CNT-CC and LRMNO@CC and the LRMNO powder sample as the cathode and Li metal anode. Half-cells fabrication has been carried out using lithium foils as both counter and reference electrodes, LRMNO@CNT-CC or LRMNO@CC as the cathode, Celgard 2400, as the separator, and 1 M $LiPF_6$ in ethylene carbonate and propylene carbonate (1:1 ratio) solution as the electrolyte, inside the Ar filled glove box. Galvanostatic charge/discharge measurements were carried out in the voltage range between 3.5 to 4.9 V at different C rates (1C = 250 mA h g^{-1}) using Neware BTS 4000 multi-channel battery tester coupled with BTS 8.0. software. Cyclic voltammetry (CV) measurements were carried out in the voltage range between 3.5 to 4.9 V (vs. Li/Li^+) using CorrTest EC Studio electrochemical workstation (Ver.5.6).

S.1. 5. Flexible Lithium-ion pouch cell preparation using Li-rich cathode materials

The Li-rich cathode materials LRMNO@CC and LRMNO@CNT-CC have been tested for their fuel cell performance by preparing a pouch cell. To construct the flexible lithium-ion pouch cell, the Mn_3O_4 nanoparticles prepared by the solution route, deposited on carbon fibers (MO@CC) were used as the anode in couple with the 3D LRMNO@CNT-CC or LRMNO@CC cathode and sealed inside an Al/polyethylene film. The assembly has been carried out in an Ar-filled glove box for a controlled atmosphere. The LRMNO@CC and LRMNO@CNT-CC fabrics were arranged on the aluminium sheets one above the other, well separated by the Celgard separator. The Celgard separator wrapped properly on both sides of the flexible aluminium sheet to avoid the contact between the electrodes. The LRNMO cathode and the surface of the separator were wetted by the $LiPF_6$ mixed with EC+PC (1:1 M) electrolyte. An insulation tape properly bound the elongated contacts of the aluminium sheets to avoid contact between the electrodes. The assembled pouch cells are highly flexible, bendable in any direction, if any contact between the cathode and anode inside the cell is avoided. The fuel cell was charged and discharged between 2.5 and 3.8 V at different C rates. The calculation of the specific capacities for both half-cells and fuel cells were based on the active mass of LRMNO. The mass loadings were measured using a Sartorius Analytical balance (CPA225D, with a resolution of 10 μg).

S2. Structural features of LRMNO nanoparticles

The Li_2MnO_3 (LRMO) cathode materials are considered as a source of attraction due to their very high theoretical capacity (452mAh/g). The Ni incorporation, in LRMO, without changing the structure (LRMNO) needs fine tuning of composition, morphology, microstructure and surface properties of the active material. The present study attempted different compositions and temperatures for the preparation of LRMNO with high electrochemical properties and maintaining the parent monoclinic phase of LRMO with C2/m phase group. The figure S1.

shows comparison of the XRD pattern of LRMNO prepared at two different temperatures 750 °C and 800 °C respectively. Even though most of the peaks are common, the LRMNO nanoparticles prepared at 800 °C have less intensive peaks confirming a transformation from the C2/m phase with the serious changes in the Li-rich layer and in the oxygen redox activities[1, 2]. The low temperature preparation results in stacking disorders and mismatches in the lattice arrangements, that results in low electrochemical performance of the material. Hence, the sample prepared at optimum temperature 750 °C maintaining the structure of the parent compound has been selected to further record its morphological tuning and electrochemical analysis. The XRD pattern of the LRMNO monoclinic C2/m phase bears a crystallite volume of 207.79 $Å^3$ with lattice parameters: a= 5.024 (Å), b=8.72 (Å), c=5.029 (Å), and β=109.45°

.

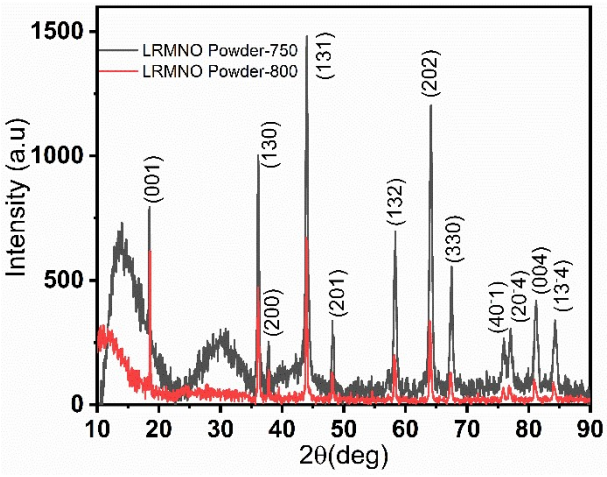

Figure S1. The XRD pattern of the LRMNO nanopowder prepared at750 and 800 °C.

S.3. Additional details on the Morphological analysis of the LRMNO@CC and LRMNO@CNT-CC samples.

The carbon network containing 3D-Vertical CVD-CNT and the crystallized GO network, provides a conduction path for the Li-rich cathode materials facilitating Li ion intercalations[3].

The figure S2 provides some additional images of the well-organized pattern of 3D vertical MWCNT derived from CVD preparation on carbon fabrics at different magnifications.

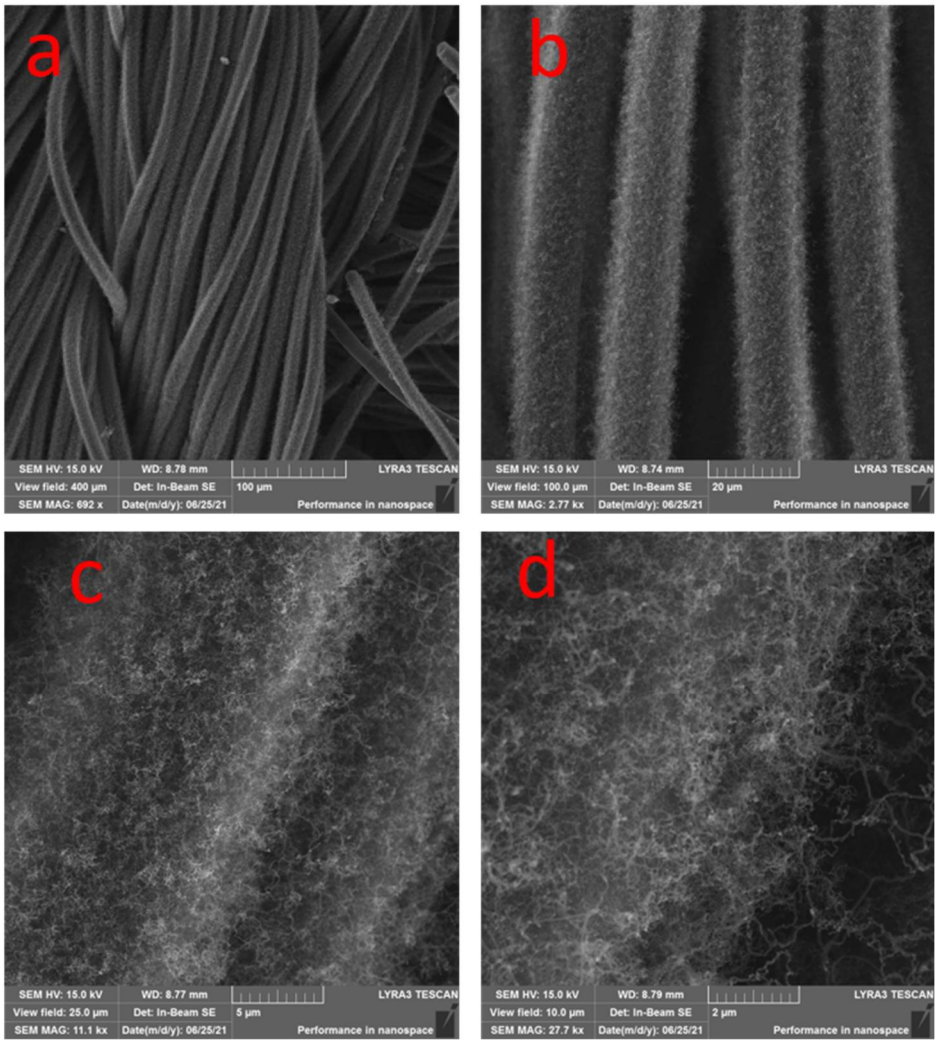

Figure S2. The SEM micrographs of vertically aligned 3D –MWCNT prepared by CVD method at different magnifications.

S.3.1. EDX Mapping of CNT-CC

The EDX mapping of bare CNT-CC prepared by CVD technique has been provided below. The sample shows uniform distribution of C all over the surface.

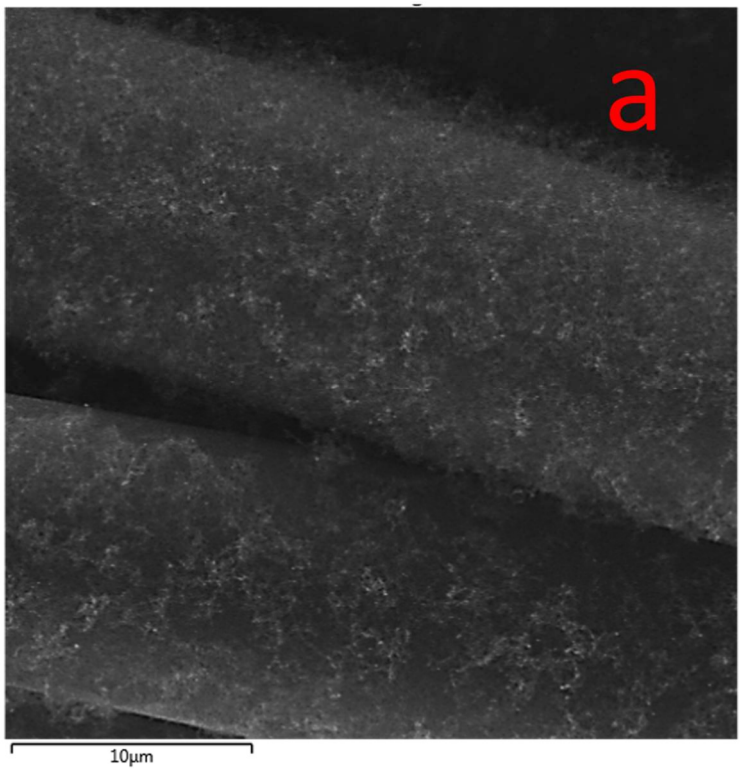

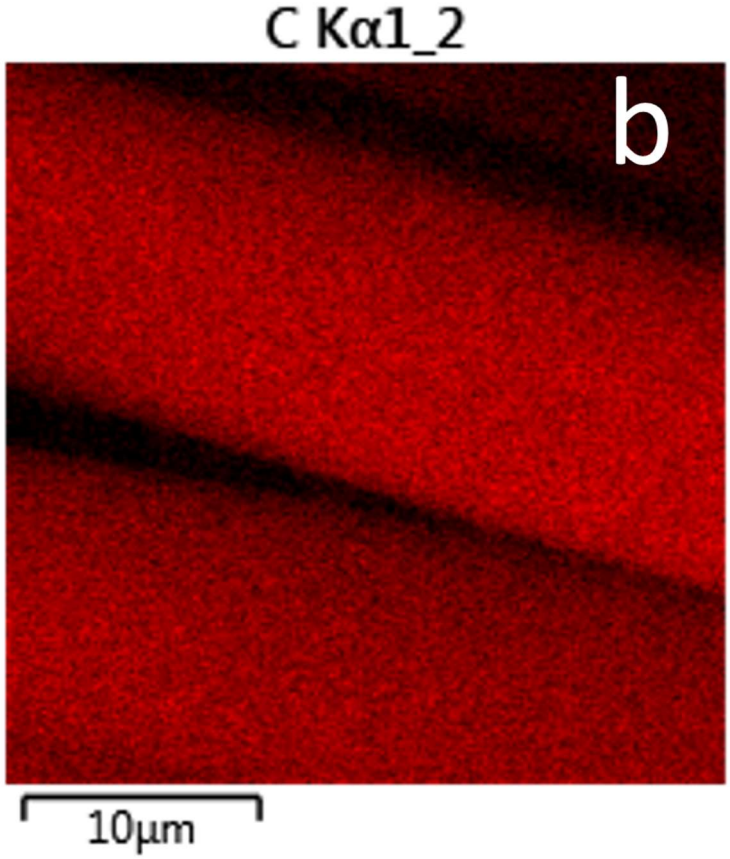

Figure S3. The SEM micrograph (a) and elemental mapping (b) of CNT@CC.

S.3.2. The STEM micrographs of 3D-vertical CNT-CC and LRMNO@CNT-CC

The STEM micrographs of the 3D–CNT array grown on the surface of a single fabric string and additional images of LRMNO@CNT-CC at different magnifications have been provided in figure S4 and S5. The CVD grown CNTs vertically aligned on the surface of carbon fibers are clearly perceptible from the white and dark field STEM micrographs of CNT-CC. The figure S5 shows the uniform arrangement of LRMNO nanoparticles arranged on the surface of 3D vertical CNTs.

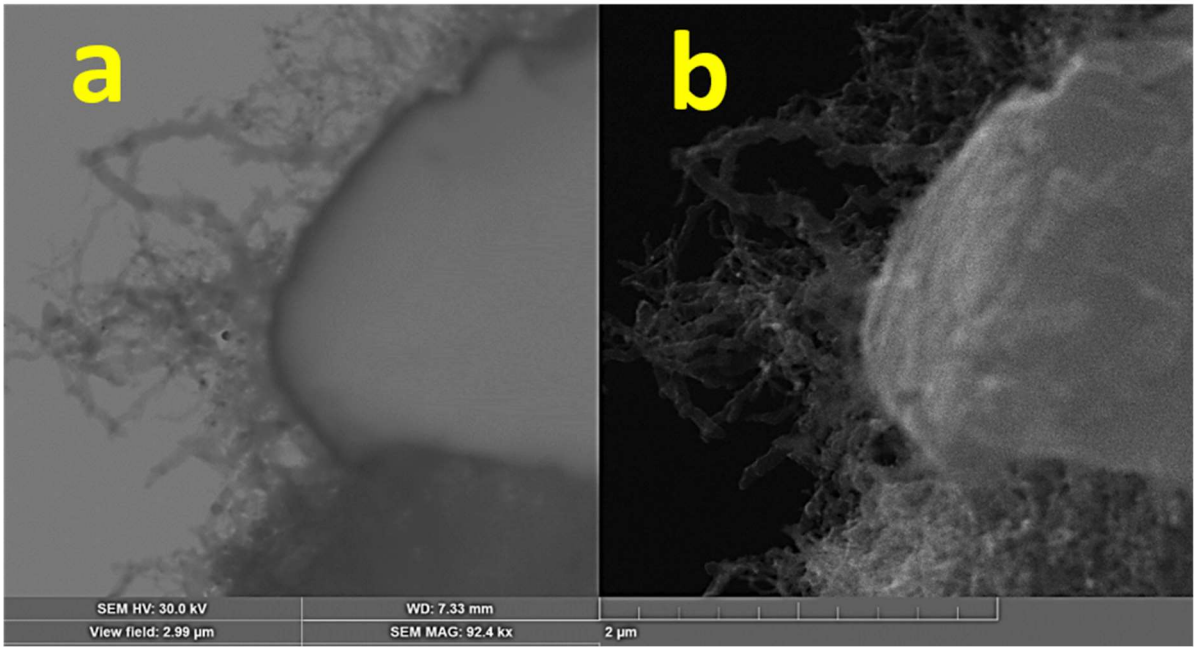

Figure S4. White (a) and dark (b) field STEM images of CVD-grown CNT-CC.

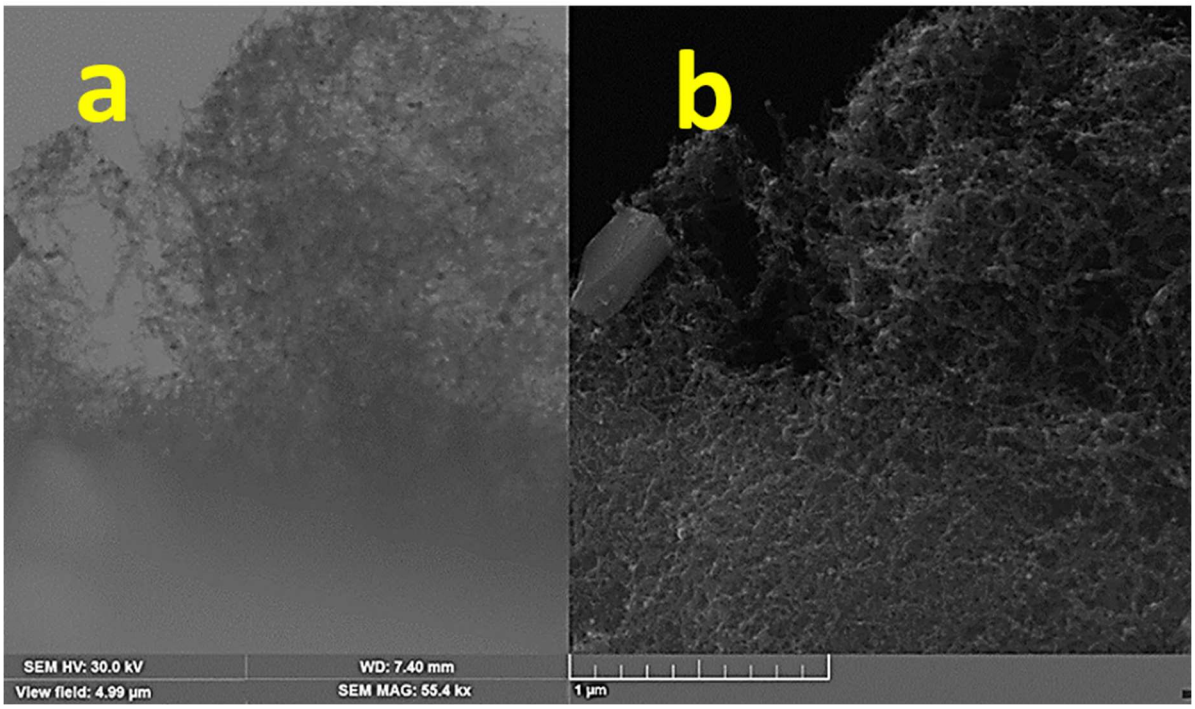

Figure S5. White (a) and dark (b) field STEM images LRMNO@CNT-CC.

S.4. The Transition Metal (TM) composition ratio in the LRMNO cathode materials

Various TM concentrations in the Li-rich cathode materials result in different phases and distinct electrochemical properties. The present study outlined a preparation of the Li-rich Ni-incorporated manganese oxide (LRMNO) which intrinsically maintains the structure of the Li_2MnO_3 monoclinic C2/m phase. Variations on the TM (Ni and Mn) concentration have been attempted in the present study. The desired composition with exceptional electrochemical properties has almost equal TM ion concentrations (Ni/Mn ratio almost 0.90-0.93). The LRNMO nano-powder prepared at two different temperatures (750 °C and 800 °C), and the nanoparticles-spray-coated LRMNO@CC and LRMNO@CNT-CC have been examined for their elemental composition, in which all the samples except the LRMNO powder prepared at 800 °C keep the Ni/Mn ratio within the range 0.90 to 0.93. This substantiates the stoichiometric composition for the preparation of the compound $Li_2(Mn_{0.5}Ni_{0.5})O_3$ intrinsically maintaining the C2/m phase with interesting electrochemical properties.

Table S1: The weight percentage obtained from the elemental analysis (EDX) of different LRMNO samples and atomic ration of these two metals.

Samples	Mn (Wt%)	Ni (Wt%)	At. Ni/Mn
LRMNO Powder sample (Prepared at 800◦C)	20.0	16.4	0.77
LRMNO Powder sample (Prepared at 750◦C)	20.3	20.1	0.93
LRMNO@CC	18.2	17.4	0.90
LRMNO@CNT-CC	12.3	12.1	0.92

S.5. The integral area calculation within the D and G spectral lines of the Raman Spectra

The Raman spectra can be employed to identify the purity, degree of crystalline carbon and defects content in the sample[4]. The spectral band occurring at around 1345 cm^{-1} (D band), is highly sensitive to the defects in the graphitic sp^2 carbon network typical for carbon-related impurities together with the amorphous carbon particles. The D band originates from the defect-related sp^3 hybridized carbon networks. The spectral band at around 1580 cm^{-1} (G band), originates from the highly graphitic sp^2 carbon network. The area under the G and D band and the intensity ratio of the band (I_G/I_D) indicate the ordered carbon network within the sample and thus the crystalline carbon components in the CC, CNT@CC, LRMNO@CC, LRMNO@CNT-CC samples.

The integral area has been calculated using the Origin software after subtracting the spectral background of the sample. The degree of the graphitic carbon content can be calculated using the formula:

$$C_G = A(G)/A(G)+A(D) \quad (1)$$

The LRMNO@CNT-CC sample exhibits defects and sp^3 hybridized carbon atoms in ordered sp^2 carbon network of CNT. The ratio of defect related D band and sp^2 hybridized carbon atoms from G band is typically for CVD growth multiwall carbon nanotubes network.

The post-cycling analysis of the Raman spectra suggests that the graphitic components are highly diminished in the LRMNO@CC samples compared to the LRMNO@CNT-CC sample, which keeps the characteristic D and G fingerprints even after the long-term cycling (up to 1000 cycles). The integral area under the G and D peaks, intensity ratio, and the graphitic carbon components of the LRMNO@CNT-CC and LRMNO@CC samples have been included in table S2.

Table S2. The Post-cycling Raman parameters (intensity ratio, integral area, full width half maximum (of D and G peaks) and the calculated crystalline percentage of carbon) derived from the D and G peaks of the Raman spectra of LRMNO@CC and LRMNO@CNT-CC samples.

Sample	I_G/I_D	Integral Area of		FWHM		Crystalline percentage of carbon (%)
		G band	D band	D	G	
		A(G)	A(D)			A(G)/[A(G)+A(D)]
LRMNO@CNT-CC	0.999	684.07	1416.9	57.94	50.84	32.55
LRMNO@CC	0.998	2362.7	3530.8	103.9	68.71	40.10

S.6. XPS analysis of LRMNO powder

The XPS analysis has been used to probe the amount of Mn^{3+} and Mn^{4+} bonding states from the peak multiplet, which were 34.3, and 65.7 % respectively (figure S3). The extrusive Mn^{3+} concentration in the prepared LRMNO nanoparticles warrants superior electrochemical activity of the sample when compared to the parent LRMO samples, which contain

electrochemically less active saturated Mn^{4+} components[5]. The C 1s spectrum was deconvoluted into five binding states: C=C, C-C, C-O, C=O and O=C-O with proportions of 76.7, 14.1, 3.7, 3.9 and 1.6 %, respectively. The survey spectrum shows the presence of Li, Ni, Mn, O and C components as shown in figure S4. The Li 1s peak is found to be overlapped with the Mn 3p peak as shown in figure S4.

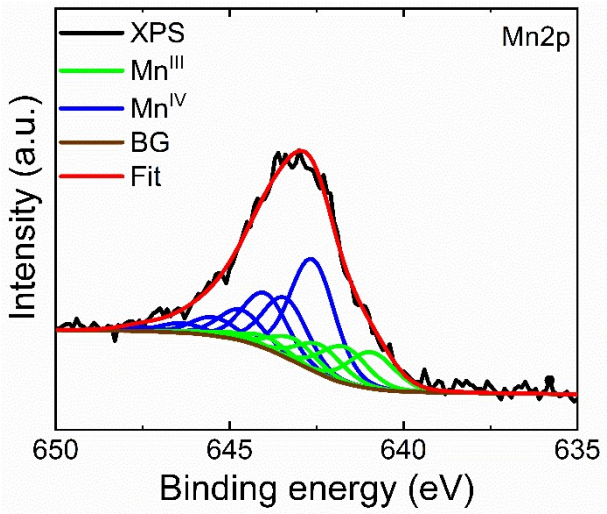

Figure S6. The Mn^{3+} and Mn^{4+} peak intensity resolving.

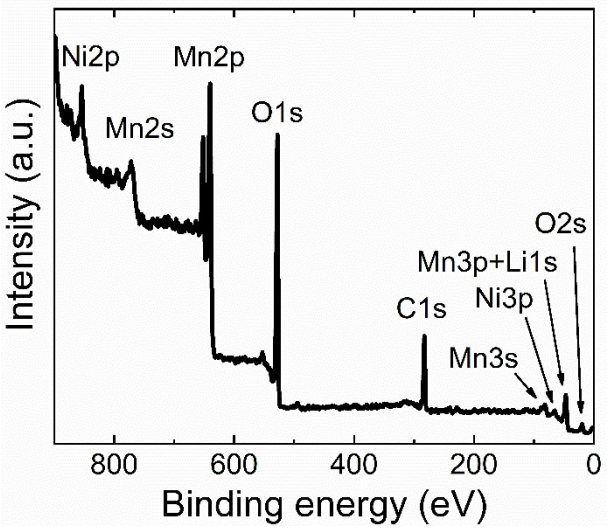

Figure S7. The survey spectrum of LRMNO nanoparticles.

S.7. Electrochemical analysis of the bare LRMNO powder

The Li-rich LRMNO powder sample has been prepared at different temperatures and different TM compositions. Among these, the samples prepared at 750 °C and 800 °C exhibit exceptional electrochemical properties. The sample prepared at 750 °C exhibits limited fading in the capacity when compared with the sample prepared at 800 °C. The figure S5 compares the capacity vs cycle number plots for the initial 100 cycles of the LRMNO samples prepared at 750 °C and 800 °C. The bare LRMNO nanopowder without any carbon support exhibits comparatively lower capacity and more fading in its capacity value than the sample prepared on the carbon fabrics or CVD-CNT-grown carbon fabrics.

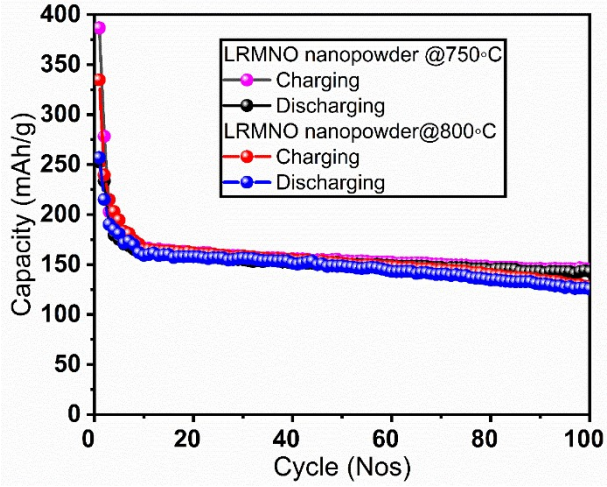

Figure S8. The capacity vs cycle number plot for the bare LRMNO powder sample prepared at 750 °C and 800 °C.

REFERENCES:

1. G.-H. Lee, V. W.-h. Lau, W. Yang and Y.-M. Kang, *Advanced Energy Materials*, 2021, **11**, 2003227.
2. Y. Cai, L. Ku, L. Wang, Y. Ma, H. Zheng, W. Xu, J. Han, B. Qu, Y. Chen, Q. Xie and D.-L. Peng, *Science China Materials*, 2019, **62**, 1374-1384.
3. A. Choi, K. Palanisamy, Y. Kim, J. Yoon, J.-H. Park, S. W. Lee, W.-S. Yoon and K.-B. Kim, *Journal of Alloys and Compounds*, 2014, **591**, 356-361.
4. A. I. López-Lorente, B. M. Simonet and M. Valcárcel, *Analyst*, 2014, **139**, 290-298.
5. T. E. Mabokela, A. C. Nwanya, M. M. Ndipingwi, S. Kaba, P. Ekwere, S. T. Werry, C. O. Ikpo, K. D. Modibane and E. I. Iwuoha, *Journal of The Electrochemical Society*, 2021, **168**, 070530.